Electronic structure of the ternary Zintl-phase compounds $Zr_3Ni_3Sb_4$, $Hf_3Ni_3Sb_4$, and $Zr_3Pt_3Sb_4$ and their similarity to half-Heusler compounds such as ZrNiSn

P. Larson
Department of Physics, Case Western Reserve University, Cleveland, Ohio 44106, USA

S. D. Mahanti
Department of Physics & Astronomy, Michigan State University, East Lansing, Michigan 48824, USA

J. Salvador and M. G. Kanatzidis
Department of Chemistry, Michigan State University, East Lansing, Michigan 48824, USA

(Received 12 May 2006; revised manuscript received 1 June 2006; published 18 July 2006)

The Zintl-phase compounds $Zr_3Ni_3Sb_4$, $Hf_3Ni_3Sb_4$, and $Zr_3Pt_3Sb_4$, are the first compounds discovered in this crystal structure not to contain Y or an *f*-electron atom. We have attempted to understand their electronic structure by comparison to the more extensively studied half-Heusler compounds such as ZrNiSn. While the half-Heusler compounds have more ionic bonding in its stuffed-NaCl crystal structure compared to the covalent Zintl network, several similarities were found between the calculated electronic structures. These similarities include the nature of the bonding, the formation of the ternary compound by adding Ni (or Pt) atoms into the octahedrally coordinated pockets of a known binary compound, and the gap formation due to Ni (or Pt) *d*-Zr *d* hybridization.

DOI: 10.1103/PhysRevB.74.035111 PACS number(s): 71.20.Nr, 72.20.Pa, 61.50.Ah

I. INTRODUCTION

Compounds in the half-Heusler structure have recently been of both theoretical and experimental interest.[1–5] Its crystal structure (*F-43m*, No. 216) can be described as a stuffed NaCl structure where transition metal ions form a fcc lattice within the pockets of the NaCl parent structure (Fig. 1).[1,2] With different chemical constituents within the structure, half-Heusler compounds can display semiconducting,[1,2] half-metallic,[3] or metallic behavior.[4] The narrow gap semiconductors of this class have been studied for thermoelectric applications.[5] The efficiency of a thermoelectric material depends on a dimensionless figure of merit $ZT=S\sigma^2T/\kappa$.[6] While the half-Heusler materials have respectable values for their thermopower (S) and electrical conductivity (σ) which lead to a large power factor ($PF=S\sigma^2$), due to their simple, isotropic (fcc) crystal structure, their thermal conductivities κ have been fairly large.[5,7–10]

Attempts to reduce the thermal conductivity through alloying have proven only moderately successful since the power factor has been observed to also reduce with alloying.[5,7–10] The large values of κ in the half-Heusler alloys have proven to be the major difficulty in using these materials for thermoelectric devices. A similar class of materials, ternary Zintl-phase compounds in the structure $Y_3Au_3Sb_4$, contain several of the same elements as the half-Heusler compounds, have similar bonding and gap formation characteristics, but, due to their cagelike structure and complex unit cells, have a low κ.[5] Other Zintl-phase compounds, such as $YbZn_2Sb_2$,[11] $Yb_{14}MnSb_{11}$,[12] and $Yb_8Ge_3Sb_5$ (Ref. 13) have been found to exhibit large power factors and low κ values at high temperatures, some better than SiGe alloys.[11,12] The materials in the $Y_3Au_3Sb_4$ structure have not been studied for their thermoelectric properties. In this paper we will show that the electronic structure of $Zr_3Ni_3Sb_4$, $Hf_3Ni_3Sb_4$, and $Zr_3Pt_3Sb_4$ have many similarities to that of the half-Heusler compounds such as ZrNiSn. The existence of anisotropic masses in the conduction band along with lower κ values due to the more complex crystal structure make this material worth investigating for thermoelectric applications.

This paper will be organized as follows: First, the crystal structure of these ternary Zintl-phase compounds will be discussed followed by the method of calculation. Next, the electronic structures of $Zr_3Ni_3Sb_4$, $Hf_3Ni_3Sb_4$, and $Zr_3Pt_3Sb_4$ will be compared to each other and to that of the half-Heusler compounds. A discussion of the observed band gaps in the half-Heusler and in this class of Zintl-phase compounds will conclude the paper.

II. CRYSTAL STRUCTURE

Zintl ions and Zintl phases have been studied for over a century,[14] but only a few of these compounds have been studied extensively. Zintl phases have been considered the "transition between metallic and ionic bonding"[15] in that the bonding, while polar in nature, is much stronger than simply

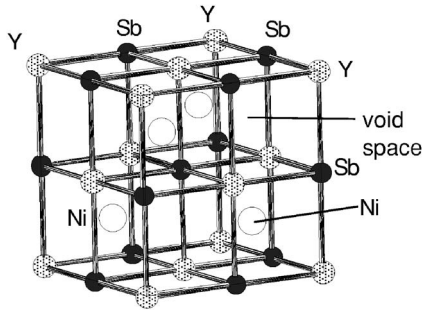

FIG. 1. Half-Heusler crystal structure of YNiSb where Ni atoms are inserted into a YSb NaCl-type lattice.

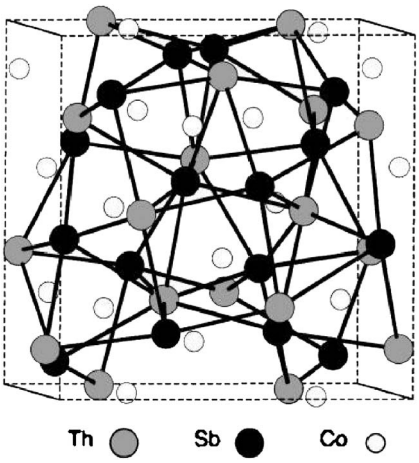

FIG. 2. Crystal structure of $Th_3Co_3Sb_4$. The Th_3Sb_4 network is shown by the heavy lines with the Co atoms lying within the voids left by this network.

ionic (often called heteropolar). These materials are defined by forming in "nonmetallic" crystal structures with complex structures having complicated atomic coordination. Due to the coordination of the anions, valence electrons are transferred from the metal atom to a more noble metal leading to strong ionicity in the metal bond.[16] Zintl ions are clusters or aggregates of "polar" intermetallic ions with strong charge transfer or covalent bonding between elements. Zintl phases form out of Zintl ions arranged to produce polar or saltlike, binary or ternary compounds formed between alkali or alkali-earth elements and the main-group elements from group IV on. Most of these compounds are either semiconductors or semimetals due to the inherent charge balance necessary for their formation.[17,18]

Zintl-phase compounds of the form $Y_3Au_3Sb_4$ (*I-43d*, No. 220) are understood as a stuffed Th_3P_4 structure. Cubic Y_3Sb_4 (Th_3P_4 structure) derives from doubling the unit cell of bcc Sb (2 Sb atoms/unit cell) in all three directions to produce a Sb supercell (16 Sb atoms/unit cell). The Sb atoms are then displaced slightly along the 111 direction of the supercell to produce two different types of Sb polyhedra: regular disphenoids[19] and distorted tetrahedra. The Y atoms enter the center of the disphenoids and are eightfold coordinated to Sb to form Y_3Sb_4 (Fig. 2). The noble (or transition) metal atoms, such as Au, enter the distorted tetrahedra sites of Y_3Sb_4 to form the ternary compound $Y_3Au_3Sb_4$ (Fig. 2). After Au is added, Y is fourfold coordinated to Sb and fourfold coordinated to Au, Au is fourfold coordinated to Y and fourfold coordinated to Sb, and Sb is threefold coordinated to Au and fourfold coordinated to Y. This resembles the formation of the half-Heusler compounds in which, such as in YNiSb, Ni atoms order themselves within the pockets of the NaCl structure of YSb. (Fig. 1). In these compounds Ni is fourfold coordinated to Y and fourfold coordinated to Sb, and the Ni-Sb and Ni-Y distances are the same. However, in the $Y_3Au_3Sb_4$ structure, due to the distortions of the tetrahedra, the different coordinations of the elements are at slightly different distances.[20]

The $Y_3Au_3Sb_4$-type Zintl-phase and half-Heusler compounds share many similarities including the formation of their crystal structure from parent binary structures and the nature of the opening of their band gaps.[21–23] Both of these structures contain a backbone compound which is predicted to be either semiconducting or semimetallic (such as ZrSn or Zr_3Sb_4) where transition (or noble) metal atoms enter into the octahedrally, coordinated pockets of this parent compound. It is important to note, however, that the bonding in the parent compounds of these two classes of materials is quite different. The crystal structure of the half-Heusler compounds formed from adding a Ni atom to the NaCl parent compound is shown in Fig. 1. In both the half-Heusler and Zintl phases, Ni is octahedrally coordinated to 4 Zr and 4 Sb atoms and 4 Ni atoms form a tetrahedra about the Zr atoms. However, there is a fundamental difference between these two structure types in regard to the Ni coordination with Sn/Sb. In the half-Heusler phase, Ni forms tetrahedra about Sn, but in these Zintl phases there are only 3 Ni atoms about the Sb positions, even though the corresponding Ni-Sb-Ni angle (114.88°) is close to the tetrahedral angle. This difference in local coordination changes the nature of the bonding between these two classes of materials and may be the reason why certain noble or transition metals appear to prefer one structure over the other. While Ni prefers to form semiconductors in the half-Heusler structure, Cu forms more stable semiconducting compounds in the Zintl-phase configuration for $R_3Cu_3Sb_4$ (R=Y, La, Ce, Pr, Nd, Sm, Gd, Tb, Dy, Ho, and Er).[23] In fact, some of the U-containing compounds can be in either phase (UNiSn and $U_3Ni_3Sb_4$, UPtSn and $U_3Pt_3Sn_4$, URhSb and $U_3Rh_3Sn_4$).[23]

The search for new thermoelectric materials involves finding new narrow-gap semiconductors.[6] Metallic Zintl compounds, such as $Th_3Co_3Sb_4$,[24] have low thermopower values (typical for metals) though there is an expectation of a reduction in the lattice thermal conductivities. Several semiconducting members of this class of Zintl compounds have been found and studied experimentally.[20–23,25–27] $Th_3Ni_3Sb_4$ (Ref. 25) has been found both experimentally and theoretically to be a narrow-gap semiconductor. Both $U_3T_3Sb_4$ (T=Ni, Pd, Pt) (Ref. 26) and $Ce_3Pt_3Bi_4$ (Ref. 21) are heavy-fermion, narrow-gap semiconductors with magnetic moments on the U and Ce sites, respectively. However, these heavy-fermion, narrow-gap semiconductors do not have large thermoelectric coefficients at room temperature.[28]

$Zr_3Ni_3Sb_4$, $Hf_3Ni_3Sb_4$, and $Zr_3Pt_3Sb_4$ were identified by Wang *et al.*[27] to have the same crystal structure as the better studied $Y_3Au_3Sb_4$ structure type not containing Y or an *f*-electron atom. As discussed for $Y_3Au_3Sb_4$, in $Zr_3Ni_3Sb_4$ Ni has 4 Zr and 4 Sb neighbors, Zr has 4 Ni and 4 Sb neighbors, and Sb has 4 Zr and 3 Ni neighbors. The shortest Zr-Sb distance is 2.9144 Å, the shortest Zr-Ni distance is 2.7746 Å, and the shortest Ni-Sb distance is 2.4858 Å.[27]

In their analysis of $Zr_3Ni_3Sb_4$, Wang *et al.*[27] claim that, in a Zintl-phase concept, Sb is considered a nonmetallic element since it is the most electronegative component. They claim the observed short Zr-Ni distance, 2.7746 Å, produces a strong covalent bonding between Zr and Ni so that $(ZrNi)_3$ forms the covalent network which then has predominantly ionic bonding with the interpenetrating Sb atoms. This picture is consistent with their extended Hüuckel calculation which showed a reduced charge on Zr. However, this de-

scription disagrees with that given by Jingtai *et al.*[29] who studied similar metallic rare-earth (RE)-copper Zintl phases $RE_3Cu_3Sb_4$. They claim that, due to the shorter Cu-Sb distance (2.630 Å compared to the Cu-RE distance of 2.868 Å), Cu_3Sb_4 forms the covalent network and the interpenetrating RE atoms, in the distorted tetrahedra of Cu_3Sb_4, have ionic bonding with the covalent Cu_3Sb_4 network. As in $Zr_3Ni_3Sb_4$, the electronegativity of Sb is larger than that of the RE atom.[29] Both Wang *et al.*[27] and Jingtai *et al.*[29] agree that there should be a strong charge transfer between Zr and Sb in $Zr_3Ni_3Sb_4$. We propose a third explanation of the Ni-based Zintl-phase compounds. Zr_3Sb_4 forms a covalent Zintl-phase network (with some charge transfer between Zr and Sb) in which the Ni atoms enter with a relatively weak hybridization between the network and the Ni *d* states which leads to the opening of a semiconducting gap, similar to that seen in the half-Heusler compounds.[1]

The lattice parameters used in the calculation were taken from experiment.[27]. Lattice relaxation was studied, but the atomic positions stayed very close to the positions dictated by symmetry and the lattice constant varied by only about 1%. There was no noticeable change in the band structure or band gaps due to the relaxation, so the experimental values were used. The lattice constants are 9.066 Å for $Zr_3Ni_3Sb_4$, 9.016 Å for $Hf_3Ni_3Sb_4$, and 9.359 Å for $Zr_3Pt_3Sb_4$. The Zr and Hf site is at the 12*a* Wyckoff position $(\frac{3}{8},0,\frac{1}{4})$, Ni and Pt at the 12*b* Wyckoff position $(\frac{7}{8},0,\frac{1}{4})$, and Sb at the 16*c* Wyckoff position (0.0827,0.0827,0.0827).[27] As has already been mentioned, lattice relaxation changed these positions very little.

In this paper we will discuss the electronic structure of three Zintl-phase compounds of the $Y_3Au_3Sb_4$ structure type, namely $Zr_3Ni_3Sb_4$, $Hf_3Ni_3Sb_4$, and $Zr_3Pt_3Sb_4$. The reasons for studying these systems is (i) to understand how the Zintl concept applies to these materials, (ii) to understand the role in the gap formation of Ni/Pt *d* hybridization compared to the half-Heusler compounds, and (iii) to understand the electronic origin of their thermoelectric properties.

III. METHOD OF CALCULATION

Electronic structure calculations were performed using the self-consistent full-potential linearized augmented plane-wave method (FLAPW) (Ref. 30) within density-functional thoery (DFT) (Ref. 31) using the generalized gradient approximation (GGA) of Perdew, Burke, and Ernzerhof[32] for the exchange and correlation potential. The calculations were performed using the WIEN97 package.[33] The values of the atomic radii were chosen to be 2.38 a.u. (a.u. =atomic unit=0.529 177 Å) in order to minimize the area between the spheres. Adjustments of these radii within a reasonable range showed little dependence of the final band structure on these variations. Convergence of the self-consistent iterations was performed with 14 **k** points for Zr_3Sb_4 and 73 **k** points for $Zr_3Ni_3Sb_4$, $Hf_3Ni_3Sb_4$, and $Zr_3Pt_3Sb_4$ within the reduced Brillouin zones to within 0.0001 Ry where RKMAX is 8 and GMAX is 10. Relativistic corrections were added in two stages. Scalar relativistic corrections were added in the self-consistent cycle directly while the spin-orbit interaction (SOI) was included using a second-variational procedure.[34]

IV. COMPARISON OF BAND STRUCTURES OF $Zr_3Ni_3Sb_4$, $Hf_3Ni_3Sb_4$, AND $Zr_3Pt_3Sb_4$

The electronic structures of all three compounds show small semiconducting gaps (Fig. 3). We find that the effect of SOI is to reduce the band gap from 0.45 to 0.39 eV in $Zr_3Ni_3Sb_4$, from 0.58 to 0.51 eV in $Hf_3Ni_3Sb_4$, and from 0.86 to 0.78 eV in $Zr_3Pt_3Sb_4$. Though extended Hückel calculations rarely do a good job in predicting band gaps, the previous calculation for $Zr_3Ni_3Sb_4$ (without SOI) gave a gap of 0.57 eV, consistent with our results.[27] There do not yet exist experimental measurements for the band gaps in these materials.

The electronic structures of $Zr_3Ni_3Sb_4$, $Hf_3Ni_3Sb_4$, and $Zr_3Pt_3Sb_4$ are remarkably similar, the valence band maxima forming along the same directions which are apparently multiply degenerate along ΓN (called $v1$), ΓH (called $v2$), and ΓP (called $v3$). (Fig. 3) These bands arise primarily from Hf/Zr *d* and Ni/Pt *d* hybridization, with some Sb *p* mixing. In each case, the effect of SOI is to remove the degeneracies from the bands and reduce the observed band gap by about 0.07 eV. As in the half-Heusler systems, the bands near the Fermi level arise due to a strong hybridization of the three elements.[1]

A closer study of the effective masses of these materials shows that there are only two valence band maxima along ΓH and ΓP in $Zr_3Ni_3Sb_4$ and $Hf_3Ni_3Sb_4$, the supposed maxima along ΓN($v1$) in these two compounds, which has a slightly lower energy than the other two, is really a saddle point with a minimum along the *x* direction (Table I). The effective mass tensor is defined as $\alpha_{ij}=\partial^2 E/\partial k_i k_j$. The energy near the band extrema can be written as[35]

$$2m_e/\hbar^2 = \alpha_{xx}k_x^2 + \alpha_{yy}k_y^2 + \alpha_{zz}k_z^2 \quad (1)$$

where m_e is the bare electron mass and a constant term has been ignored. The values of the reciprocal mass tensor have not been measured experimentally. The conduction band minimum at the Γ point is doubly degenerate, one band more dispersive than the other. The values of the reciprocal effective mass tensor are very similar, except for the heavier conduction band minima and no saddle point in the Pt compound (Table I).

V. COMPARISON OF THE BAND STRUCTURES OF $Zr_3Ni_3Sb_4$ WITH THE HALF-HEUSLER COMPOUND ZrNiSn

A. Gap formation from parent binary compounds

The gap formation in the half-Heusler compounds $Y^{3+}Ni^0Sb^{3-}$ and $Zr^{4+}Ni^0Sn^{4-}$ derives from a charge transfer between the elements of the NaCl substructure with the strong hybridization of the Ni *d* and Y/Zr *d* orbitals.[1,2] Similarly, in the Zintl-phase compounds the charge transfer in the binary parent compound $(Zr^{4+})_3(Sb^{3-})_4$ to form the ternary

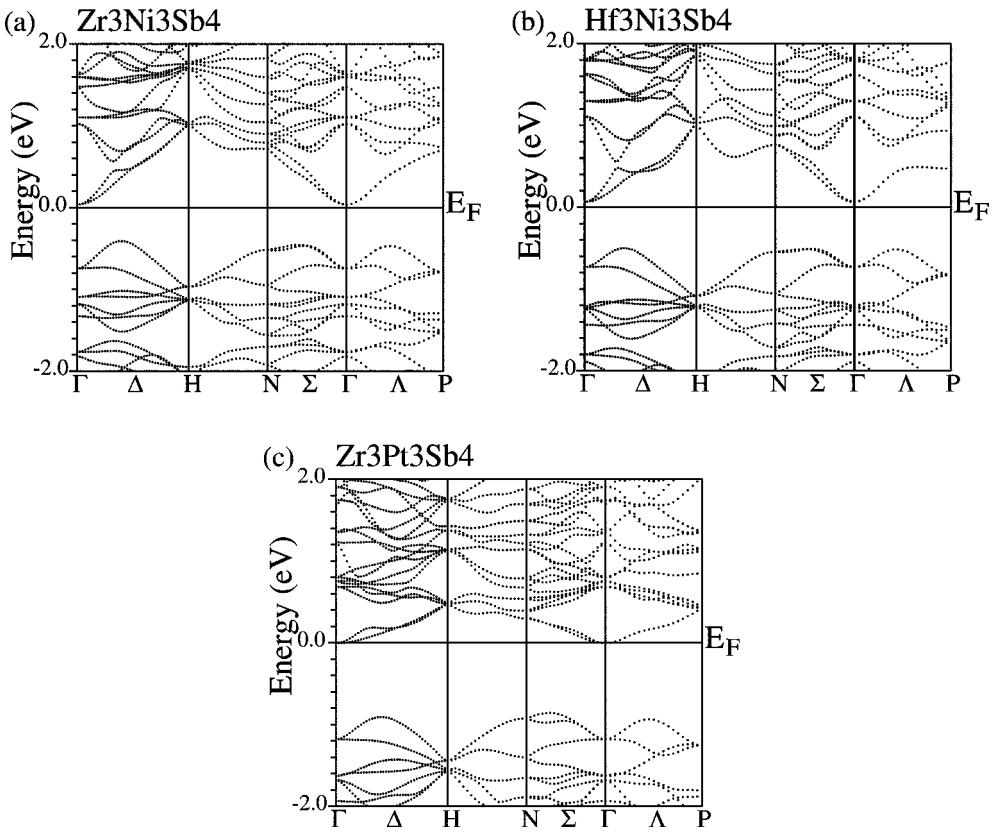

FIG. 3. Electronic structures of (a) $Zr_3Ni_3Sb_4$, (b) $Hf_3Ni_3Sb_4$, and (c) $Zr_3Pt_3Sb_4$.

$(Zr^{4+})_3(Ni^0)_3(Sb^{3-})_4$ should be important in understanding the gap formation in these materials.

Before discussing the similarities between the Zintl-phase and half-Heusler compounds, one should note the differences as well. While both of the binary parent compounds are predicted to be semimetals, different bonding is seen for these two compounds. The Zr *d* and Sn *p* orbitals in ZrSn (Fig. 4) are much more separated than the Zr *d* and Sb *p* of the covalent network in Zr_3Sb_4 (Fig. 5) where the character of both atoms are seen more prominently above and below the Fermi energy. Neither of these binary compounds have been measured experimentally. Zr and Sn have not been found to form in this cubic phase.[36] While Zr_3N_4 and Hf_3N_4 have been produced in the Th_3P_4 crystal structure under high pressures,[37,38] electrical measurements were not performed to determine whether these materials are metallic, semimetallic or semiconducting. Zr_3Sb_4 has not been produced as yet in this crystal structure.

Previous calculations have been performed on other Th_3P_4 structure materials. Some examples are the U_3P_4 (P=P, As, Sb, Bi, Se, Te) (Ref. 39) and RE_3S_4 (RE=Nd, La).[40] In these cases the rare-earth atoms provide *f* electrons which were treated with LSDA+U where Hubbard U corrections are added to the local spin-density approximation (LSDA). The anti-Th_3P_4 compounds Sr_4Bi_3, Ba_4Bi_3, and Ba_4As_3 were found to become semiconducting upon electron deficiency of the Bi or As sites.[41] The above examples are all metallic since their electron count does not balance.

In contrast to the previous examples, the electron count of the binary M_3Sb_4 (M=Zr, Hf) should exactly balance to

TABLE I. Calculated components of the effective mass tensor for the conduction band minimum (CBM) and valence band maximum (VBM) of $Zr_3Ni_3Sb_4$, $Hf_3Ni_3Sb_4$, and $Zr_3Pt_3Sb_4$.

	$\alpha_{ij}=[m_{ij}/m_e]$	$Zr_3Ni_3Sb_4$	$Hf_3Ni_3Sb_4$	$Zr_3Pt_3Sb_4$
CBM (Γ)	$\alpha_{xx}=\alpha_{yy}=\alpha_{zz}$	1.46	1.53	0.07
	$\alpha_{xx}=\alpha_{yy}=\alpha_{zz}$	0.72	0.57	0.08
VBM ($v1$)	$\alpha_{xx}=\alpha_{yy}$	0.21	0.27	0.50
	α_{zz}	−0.04	−0.23	0.54
VBM ($v2$)	$\alpha_{xx}=\alpha_{yy}=\alpha_{zz}$	0.17	0.19	0.12
VBM ($v3$)	$\alpha_{xx}=\alpha_{zz}$	0.47	0.40	0.26
	α_{yy}	1.26	1.24	0.88

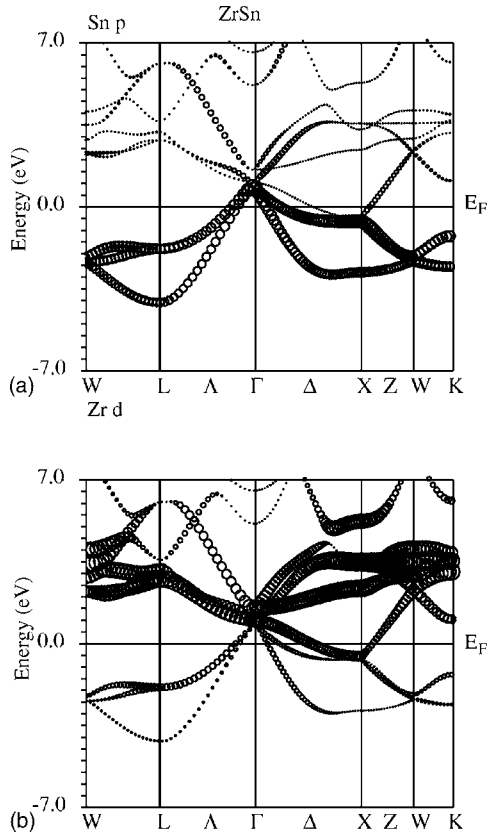

FIG. 4. The (a) Sn p and (b) Zr d orbital characters of NaCl ZrSn, the parent compound of the half-Heusler ZrNiSn. The size of the circles associated with the "fatband" representation corresponds to the orbital character of the band.

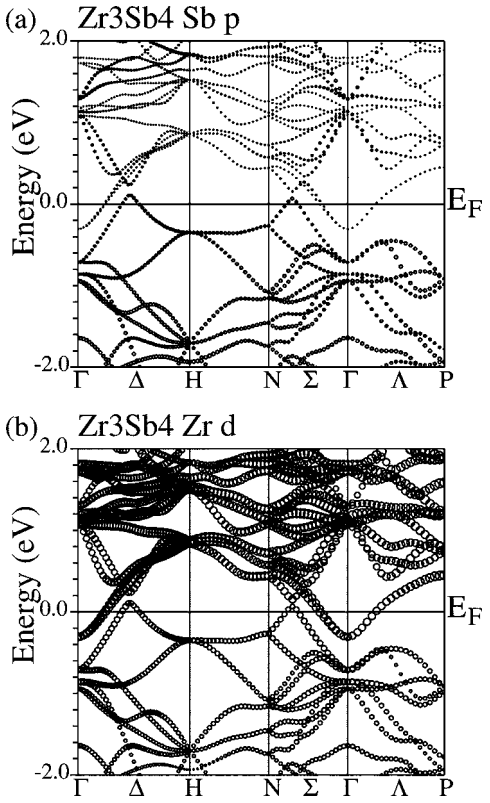

FIG. 5. The (a) Sb p and (b) Zr d orbital characters of Zr_3Sb_4. The size of the circles corresponds to the amount of the orbital character in the band. Note the similarity between the band characters in Zr_3Sb_4 and ZrSn (Fig. 4) with the Zr d above and Sb p below E_F forming a semimetal.

form a semiconductor. We will show that it is weakly semiconducting, similar to the binary compound ZrSn which forms the parent compound of the half-Heusler compound ZrNiSn. Let us briefly review the gap formation in the half-Heusler compound ZrNiSn.[1,2] The gap formation in the half-Heusler compounds has been understood by first studying the parent binary compound ZrSn and then studying the effects of the inclusion of the Ni d levels in the gap formation in the ternary. The parent binary compound is semimetallic with bands crossing the Fermi level near the X point and the Γ point. In ZrNiSn the strong Ni d-Zr d hybridization in the conduction band near the X point leads to the formation of the band gap (Fig. 4).[1,2]

An understanding of the gap formation in $Zr_3Ni_3Sb_4$ comes by studying what effect the Ni d orbitals have on semimetallic Zr_3Sb_4. Using the experimental value of the lattice constant of the ternary compound,[1] we have calculated the band structure of Zr_3Sb_4 (Fig. 5). It can be seen that Zr_3Sb_4 is also slightly semimetallic with a conduction band crossing the Fermi level near the Γ point and valence bands above the Fermi level along ΓH and ΓN (Fig. 5). This is consistent with the self-consistent APW calculations for Th_3Sb_4, which is an existing compound.[25] As can be seen, the majority of Zr d bands lies above the Fermi level and the majority of the Sb p bands lies below, consistent with the view that these are mostly polar salts in the Zintl phase.[18] The important question is how the inclusion of Ni changes the bonding within this network.

Before looking at how Ni changes the band structure when added to Zr_3Sb_4, it is important to review what happens when Ni is added to ZrSn. The opening of the band gap in the half-Heusler compounds has been discussed in detail before.[1,2] The explanation by Larson *et al.*[1] showed that the Sn p states play little role in the gap formation while the Zr d and Ni d hybridization opened the band gap. Zr d states form the bottom of the conduction band with a strong Zr d character at the Γ point at the top of the valence band. Similarly, Ni d states form the top of the valence band, except near the Γ point, with a strong Ni d character at the bottom of the conduction band at X. The strong hybridization between the Ni d and Zr d states pushes up the overlapping bands at X in ZrSn (Fig. 4) to form a semiconductor in ZrNiSn.

In $Th_3Ni_3Sb_4$,[25] it has been found that the Th d-Ni d hybridization at the Γ point is much stronger than the Sb p-Ni d hybridization and that this larger hybridization leads to the formation of the semiconducting gap. This is true even though the Ni-Sb distance (2.644 Å) is smaller than the Ni-Th distance (2.874 Å).[25] Therefore, the interatomic distance is not a clear indicator of the local bonding, as is commonly used. We also find that, when Ni is added to Zr_3Sb_4 to form $Zr_3Ni_3Sb_4$, the gap formation is similar to that of the half-Heusler compounds, when Ni is added to ZrSn to form ZrNiSn. The strengths of the orbital characters in $Zr_3Ni_3Sb_4$ (Fig. 6) show that the Ni d hybridizes more strongly with Zr d than with Sb p. The Zr d-Ni d hybridization at the Γ

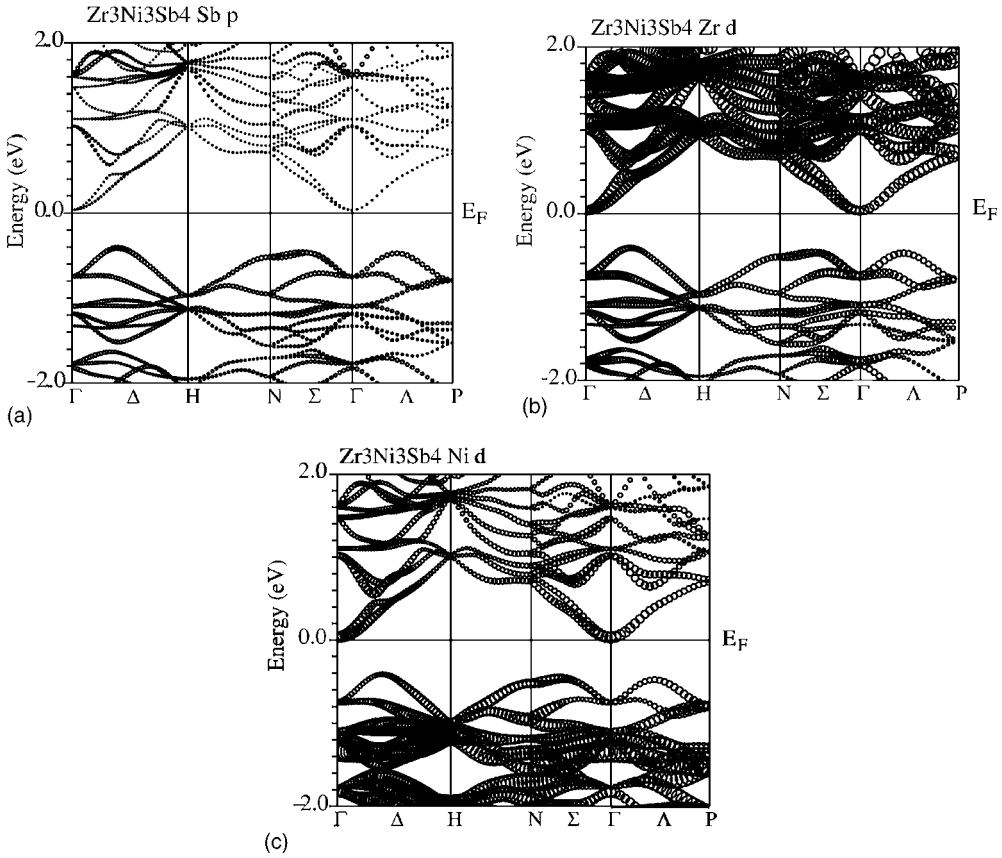

FIG. 6. The (a) Zr *d*, (b) Sb *p*, and (c) Ni *d* orbital characters of $Zr_3Ni_3Sb_4$. Again, the size of the circles corresponds to the amount of orbital character. The orbital character for Zr *d* and Sb *p* is almost the same as in Zr_3Sb_4 (Fig. 5), but the Ni *d* states hybridize with the Zr *d* to open a band gap.

point is much stronger than the Sb *p*-Ni *d* hybridization and this leads to the formation of the semiconducting gap in $Zr_3Ni_3Sb_4$. The conduction band which dips below E_F Zr_3Sb_4 [Fig. 5(b)] hybridizes with the Ni *d* states [Fig. 6(c)] and is pushed up [Fig. 6(b)], opening a gap as in the half-Heusler compounds. Again, the Ni-Sb distance (2.4858 Å) is smaller than the Zr-Ni distance (2.7746 Å).

B. Unusual discrepancy between the band gaps from theory (LDA/GGA) and experiment

As in the half-Heusler structure, there seems an unusual discrepancy between the experimental and theoretical band gaps, the theoretical values being much larger than the experimental values,[1,2,25] the opposite of what is usually found in LDA/GGA calculations.[42] The band gaps have not been measured in $Zr_3Ni_3Sb_4$, $Hf_3Ni_3Sb_4$, or $Zr_3Pt_3Sb_4$, but a comparison can be made with calculations and experiments in the literature of materials in the same crystal structure. The situation seems even more confusing due to the comparisons of the electronic structure calculations of the binary compounds Th_3X_4 (X=P, As, Sb) with the ternary $Th_3Ni_3Sb_4$. The calculated band gap for the binary system Th_3P_4 by Takegahara *et al.*[25] gives 0.007 eV compared to the experimental value of 0.40 eV, whereas in Th_3As_4 they find 0.05 eV compared to the experimental value of 0.43–0.44 eV. For Th_3Sb_4 they find a negative gap (semimetal) compared to the experimental value of 0.48 eV. The reason for this discrepancy was attributed to the inadequate treatment of the exchange correlation potential in LDA/GGA. The trend for the band gaps in the ternary compounds is just the opposite. The calculated value of the gap for the ternary $Th_3Ni_3Sb_4$ is 0.37 eV compared to the experimental value of 0.07 eV. These calculations were performed without the inclusion of SOI which can be important for heavy atoms such as Th and are likely to play an important role in changing the band gap.[25]

The discrepancy of finding a larger band gap in a band structure calculation than found experimentally has also been seen in the half-Heusler compounds.[1,2,43] Ogut and Rabe[2] tried to explain the observed smaller values of the band gap in ZrNiSn by invoking disorder in the ZrSn lattice. (A recent theoretical study of the energetics of this type of disorder[44] leaves unresolved questions concerning why this particular type of disorder forms.) Similar arguments have also been put forward to explain the observed smaller gap in these Zintl-phase compounds.[25] While disorder of the ZrSn lattice has been seen in ZrNiSn,[45] there is no experimental evidence of disorder in these Zintl-phase compounds, such as $Zr_3Ni_3Sb_4$, where the Zr and Sb sites are not equivalent, which is the reason that the overestimation of the band gap is not clear in these Zintl-phase compounds. More experiments are needed to see if structural disorder may play a role, as in

the half-Heusler compounds, or if another explanation is needed.

VI. SUMMARY AND CONCLUSIONS

$Zr_3Ni_3Sb_4$, $Hf_3Ni_3Sb_4$, and $Zr_3Pt_3Sb_4$ have a low κ due to their complex unit cells.[27] Our calculations also show anisotropic effective masses, though much less anisotropic than in the half-Heusler compounds.[1,2] As pointed out for $Y_3Au_3Sb_4$ and $Y_3Cu_3Sb_4$,[20] the multiply degenerate valence band maxima away from the high symmetry points leads to a large thermopower in these systems.[46,47] The different values of the band gaps allows for shifting the temperature range at which the materials are useful.[48] These Zintl-phase compounds have promising power factors, however with a much lower κ due to their complex unit cells.[27] Further experimental studies of these materials for their thermoelectric properties is warranted.

The application of the Zintl concept in these Ni-based materials differs from those containing Cu or Au since the Ni enters as a d^{10} into the Zr_3Sb_4 network. The binary compound is already a Zintl-phase compound with strong covalent bonding between the constituent atoms. Ni enters the distorted tetrahedra sites which then weakly hybridizes with the existing network. This cannot be described as ionic since there is no charge transfer between Ni and the binary network. This hybridization is important in moving apart the Sb *p* and Zr *d* states, changing from a semimetallic state to a semiconductor.

The physics of the gap formation in the half-Heusler and the $Y_3Au_3Sb_4$-structure Zintl-phase compounds is very similar: the introduction of Ni atoms into the semimetallic binary compounds results in strong Ni *d*-Y/Zr *d* hybridization, which opens a narrow band gap (ZrSn, YSb, or Zr_3Sb_4).[1] Since Zr, Sb, Sn, and Ni are not heavy elements, the inclusion of SOI has only a small effect on the band structure, such as minor splitting of the degenerate bands and a small reduction of the band gap with no change in the shape of the lowest conduction band or highest valence band.

Another similarity between the half-Heusler and Zintl-phase compounds is the larger band gaps found in the calculation compared to experiment while the binary parent compounds have smaller gaps than the experiment, the latter consistent with LDA/GGA calculations. While this discrepancy has been attributed to disorder in the atoms in the binary parent compounds,[2,25] it is unclear what the reason may be in the Zintl-phase compounds. Further study of a possible disorder is needed for these materials.

ACKNOWLEDGMENTS

Supported by the office of Naval Research and DARPA through Grant No. N00014-01-1-0728.

[1] P. Larson, S. D. Mahanti, S. Sportouch, and M. G. Kanatzidis, Phys. Rev. B **59**, 15660 (1999).
[2] S. Ogut and K. M. Rabe, Phys. Rev. B **51**, 10443 (1995).
[3] S. J. Youn and B. I. Min, Phys. Rev. B **51**, 10436 (1995); H. Ebert and G. Schutz, J. Appl. Phys. **69**, 4627 (1991); E. Kulatov and I. I. Mazin, J. Phys.: Condens. Matter **2**, 343 (1990).
[4] G. J. Mcmullen and M. P. Roy, J. Phys.: Condens. Matter **4**, 7095 (1992); A. K. Solanki, A. Kashyap, S. Auluck, and M. S. S. Brooks, J. Appl. Phys. **75**, 6301 (1994); E. K. R. Runge, R. C. Albers, N. E. Christensen, and G. E. Zwicknagl, Phys. Rev. B **51**, 10375 (1995).
[5] *Thermoelectric Materials 2000*, edited by T. M. Tritt, G. S. Nolas, G. Mahan, M. G. Kanatzidis, and D. Mandrus, MRS Symposium Proceedings No. 626 (Materials Research Society, Pittsburgh, 2000).
[6] F. J. Disalvo, Science **285**, 703 (1999); G. Mahan, B. Sales, and J. Sharp, Phys. Today **50**, 42 (1997); T. M. Tritt, Science **272**, 1276 (1996).
[7] F. G. Aliev, N. B. Brandt, V. V. Maoschalkov, V. V. Kozyrkov, R. V. Skolozdra, and A. I. Belogorokhov, Z. Phys. B: Condens. Matter **80**, 353 (1990), and references therein.
[8] C. Uher, J. Yang, S. Hu, D. T. Morelli, and G. P. Meisner, Phys. Rev. B **59**, 8615 (1999).
[9] Y. Xia, V. Ponnambalam, S. Bhattacharya, A. L. Pope, S. J. Poon, and T. M. Tritt, J. Phys.: Condens. Matter **13**, 77 (2001); S. J. Poon, Semicond. Semimetals **70**, 37 (2001).
[10] H. Hohl, A. P. Ramirez, C. Goldmann, G. Ernst, B. Wolfing, and E. Bucher, J. Phys.: Condens. Matter **11**, 1697 (1999).
[11] F. Gascoin, S. Ottensmann, D. Stark, S. M. Haïle, and G. J. Snyder, Adv. Funct. Mater. **15**, 1860 (2005).
[12] S. R. Brown, S. M. Kauzlarich, F. Gascoin, and G. J. Snyder, Chem. Mater. **18**, 1873 (2006).
[13] J. R. Salvador, D. Bilc, S. D. Mahanti, T. Hogan, F. Guo, and M. G. Kanatzidis, J. Am. Chem. Soc. **126**, 4474 (2004).
[14] A. Johannis, C. R. Hebd. Seances Acad. Sci. **113**, 79 (1891); E. Zintl, J. Goubeau, and W. Dullenkopf, Z. Phys. Chem. Abt. A **1**, 154 (1931); F. Laves, Naturwiss. **29**, 244 (1941).
[15] H. Schäfer, B. Eisenmann, and W. Müller, Angew. Chem., Int. Ed. Engl. **12**, 694 (1973).
[16] P. C. Schmidt, Struct. Bonding (Berlin) **65**, 91 (1987).
[17] H. Schäfer, Annu. Rev. Mater. Sci. **15**, 1 (1985).
[18] J. D. Corbett, Chem. Rev. (Washington, D.C.) **85**, 383 (1995).
[19] A disphenoid is a combinatorial polyhedra which has equivalent faces and vertices with opposite edges which are congruent. These are different from the distorted tetrahedra also discussed. See H. S. M. Coxeter, *Regular Polytopes* (Pitman, New York, 1948).
[20] D. Young, K. Mastronardi, P. Khalifah, C-C Wang, R. J. Cava, and A. P. Ramirez, Appl. Phys. Lett. **74**, 3999 (1999).
[21] Z. Fisk, P. C. Canfield, J. D. Thompson, and M. F. Hundley, J. Alloys Compd. **181**, 369 (1992).
[22] M. Kasaya, K. Katoh, and K. Kakegahara, Solid State Commun. **78**, 797 (1991); K. Takegahara, H. Harima, Y. Kaneta, and A. Yanese, J. Phys. Soc. Jpn. **62**, 2103 (1993).
[23] R. V. Skolozdra, P. S. Salamakha, A. L. Ganzyuk, and O. I. Bodak, Inorg. Mater. **29**, 26 (1993).

[24] S. Sportouch and M. G. Kanatzidis, J. Solid State Chem. **162**, 158 (2001).
[25] K. Takegahara and T. Kasuya, Solid State Commun. **74**, 243 (1990); K. Takegahara, Y. Kaneta, and T. Kasuya, J. Phys. Soc. Jpn. **59**, 4394 (1990); K. Takegahara and Y. Kaneta, Prog. Theor. Phys. Suppl. **108**, 55 (1992).
[26] T. Takabatake, S-I Miyata, H. Fujii, Y. Aoki, T. Suzuki, T. Fujita, J. Sakurai, and T. Hiraoka, J. Phys. Soc. Jpn. **59**, 4412 (1990).
[27] M. Wang, R. McDonald, and A. Mar, Inorg. Chem. **38**, 3435 (1999).
[28] C. D. W. Jones, K. A. Regan, and F. J. DiSalvo, Phys. Rev. B **58**, 16057 (1998).
[29] Z. Jingtai, S. Minghu, Z. Shankang, H. Zhongle, M. Jinxiao, and M. Shaoyu, J. Rare Earths **17**, 228 (1999).
[30] D. Singh, *Planewaves, Pseudopotentials, and the LAPW Method* (Kluwer Academic, Boston, 1994).
[31] P. Hohenberg and W. Kohn, Phys. Rev. **136**, B864 (1964); W. Kohn and L. J. Sham, Phys. Rev. **140**, A1133 (1965).
[32] J. P. Perdew, K. Burke, and M. Ernzerhof, Phys. Rev. Lett. **77**, 3865 (1996).
[33] P. Blaha, K. Schwarz, and J. Luitz, WIEN97, A Full Potential Linearized Augmented Planewave Package for Calculating Crystal Properties (Karlheinz Schwarz, Techn. Universitat Wien, Austria), 1999. ISBN 3-9501031-0-4.
[34] D. D. Koelling and B. Harmon, J. Phys. C **10**, 3107 (1997), P. Novak (unpublished).
[35] N. W. Ashcroft and N. D. Mermin, *Solid State Physics* (Saunders College Publishing, Fort Worth, 1976).
[36] T. Studnitzky and R. Schmid-Fetzer, Z. Metallkd. **93**, 894 (2002).
[37] P. Kroll, J. Phys.: Condens. Matter **16**, S1235 (2004).
[38] A. Zerr, G. Miehe, and R. Riedel, Nat. Mater. **2**, 185 (2003).
[39] V. N. Antonov, B. N. Harmon, A. Ya. Perlov, and A. N. Yaresko, Phys. Rev. B **59**, 14561 (1999).
[40] V. N. Antonov, B. N. Harmon, A. N. Yaresko, and A. Y. Perlov, Phys. Rev. B **59**, 14571 (1999).
[41] B. Li, A.-V. Mudring, and J. D. Corbett, Inorg. Chem. **42**, 6940 (2003).
[42] Wilfried G. Aulbur, Lars Jonsson, and John W. Wilkins, in *Solid State Physics*, edited by H. Ehrenreich and F. Spaepen (Academic Press, Orlando, 2001), Vol. 54, p. 1.
[43] J. Tobola and J. Pierre, J. Alloys Compd. **296**, 243 (2000).
[44] P. Larson, S. D. Mahanti, and M. G. Kanatzidis, Phys. Rev. B **62**, 12754 (2000).
[45] F. G. Aliev, N. B. Brandt, V. V. Kozyr'kov, V. V. Moschalkov, R. V. Skolozdra, Yu. V. Stadnyk, and V. K. Pecharskii, Pis'ma Zh. Eksp. Teor. Fiz. **45**, 535 (1987) [JETP Lett. **45**, 535 (1987)]; F. G. Aliev, N. B. Brandt, V. V. Moschalkov, V. V. Kozyr'kov, R. V. Skolozdra, and A. I. Belogorkhov, Z. Phys. B: Condens. Matter **75**, 167 (1989).
[46] P. Larson, S. D. Mahanti, and M. G. Kanatzidis, Phys. Rev. B **61**, 8162 (2000).
[47] L. D. Hicks and M. S. Dresselhaus, Phys. Rev. B **47**, 16631 (1993); **47**, 12727 (1993).
[48] H. J. Goldsmid, *Thermoelectric Refrigeration* (Plenum, New York, 1964).